SAND2000-1898 J

6/23/00

A New Class of Octahedral Molecular Sieve Materials for the Selective Removal and Sequestration of $^{90}Sr^{2+}$

May Nyman[¶], Tina M. Nenoff[¶]*, Akhilesh Tripathi[£], John B. Parise[£,€], Robert S. Maxwell[¥], William T. A. Harrison[‡]

[¶]Catalysis and Chemical Technologies Department, M.S. 0710
Sandia National Laboratories, P.O. Box 5800, Albuquerque, N.M. 87185-0710

[£]Department of Chemistry and [€]Department of Geosciences,
State University of New York, Stony Brook, NY 11794-2100

[¥]Lawrence Livermore National Laboratory, P.O. Box 808, L-226,
Livermore, California 94551

[‡]Department of Chemistry, University of Aberdeen
Aberdeen AB24 3UE, United Kingdom

Abstract

The structure of $Na_{16}Nb_{12.8}Ti_{3.2}O_{44.8}(OH)_{3.2} \cdot 8H_2O$, a member of a new family of Sandia Octahedral Molecular Sieves (SOMS) having a Nb/Na/M^{IV} (M = Ti, Zr) oxide framework and exchangeable Na and water in open channels, was determined from Synchrotron X-ray data. The SOMS phases are isostructural with variable M^{IV}:Nb (1:50 – 1:4) ratios. The SOMS are extremely selective for sorption of divalent cations, particularly Sr^{2+}. The ion-exchanged SOMS undergo direct thermal conversion to a perovskite-type phase, indicating this is a promising new method for removal and sequestration of radioactive Sr-90 from mixed nuclear wastes.
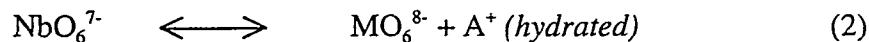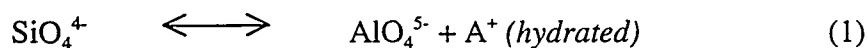
DISCLAIMER

DISCLAIMER

Portions of this document may be illegible in electronic image products. Images are produced from the best available original document.

The long term storage, containment and handling of radioactive strontium-90, cesium-137 and actinides in waste streams produced by defense-related and power generation activities pose substantial engineering, scientific, and societal challenges. The wastes containing these radionuclides are multi-component and multi-phasic. Therefore, effective ion exchangers for removal of the radionuclides must exclude competing species such as high concentrations of Na^+ (up to 5 molar solutions (*1*)) and other cations within the mixed wastes. Furthermore, appropriate ion exchangers must function in harsh chemical (highly basic or acidic) conditions, and withstand extreme radiation environments created by adsorbed radionuclides. Finally, the radionuclide-loaded ion exchanger would ideally be convertible to a stable, ceramic waste form. (*2*)

Rational design of inorganic ion exchangers for radionuclides which have tailored selectivity, high stability, and ceramic waste form capabilities holds great potential in treating such wastes. This paper reports the successful development of octahedral framework, niobate-based inorganic ion exchangers with significant selectivity for divalent ($^{90}Sr^{2+}$) cations. To synthesize an open-framework, niobate-based material, we include Ti^{IV} or Zr^{IV} oxide that can substitute into a Nb^V oxide framework and impart a net negative charge to the lattice. Further, a hydrated alkali cation functions to balance the negatively-charged framework, and simultaneously promotes the growth of an open-framework structure. This approach is analogous to substitution of Al^{III} into a $Si^{IV}O_2$ tetrahedral framework to form the aluminosilicate zeolites. Equations (1) and (2) illustrate the charge-balancing of tetrahedral-framework aluminosilicates and octahedral-framework titano(zircono) niobates, respectively:

$$SiO_4^{4-} \quad \Longleftrightarrow \quad AlO_4^{5-} + A^+ \ (hydrated) \qquad (1)$$

$$NbO_6^{7-} \quad \Longleftrightarrow \quad MO_6^{8-} + A^+ \ (hydrated) \qquad (2)$$

where A^+ is a hydrated alkali cation and M is Ti^{IV} or Zr^{IV}.

Our new niobate-based phases (*3*) only contain all octahedral framework sites, and therefore represent the first example of a new class of the octahedral molecular sieves

(OMS), previously represented by only the manganese oxide materials (*4*). These octahedral molecular sieves, unique in both their heterometallic framework and sodium framework sites, are thus named Na/Nb/M^{IV}-SOMS (M=Ti, Zr; SOMS = Sandia Octahedral Molecular Sieve) phases. Other unique features of this novel class of materials include variable Nb:M^{IV} ratio with no significant structural change, and sodium atoms occupying both octahedral framework sites and channel sites. Two of the three sodium sites are exchangeable, and furthermore, the sodium exchanges selectively for divalent cations. Both the as-synthesized and exchanged forms of Na/Nb/M^{IV}-SOMS undergo direct thermal conversion to perovskite-type phases. Finally, maximum loading of Sr^{2+} gives a 1:1 ratio of Sr^{2+}:M^{IV} (M=Ti, Zr) which upon thermal conversion, forms a charge-balanced perovskite of Na$_x$Sr$_y$Nb$_x$M$_y$O$_{3(x+y)}$. Therefore, removal of ^{90}Sr^{2+} from contaminated groundwater or nuclear waste solutions by sorption into Na/Nb/M^{IV}-SOMS, followed by direct thermal conversion to a durable perovskite phase waste form is a viable new method for ^{90}Sr^{2+} cleanup.

The SOMS phases are synthesized by hydrothermal treatment (175 °C / 5 days) of extremely basic (pH = 13.6) sol mixtures containing water, sodium hydroxide, and hydrolyzed metal (Nb, Ti, Zr) alkoxides. The M^{IV}:Nb ratio (M=Ti,Zr) in the resultant Na/Nb/M^{IV}-SOMS phase is directly correlated with the precursor ratio for the range of 1:50 – 1:4 M:Nb. Within this composition range, isostructural materials are formed, based on powder X-ray diffraction analysis. Thus, for the sake of further discussion, compositions of these phases are described as x%-Na/Nb/M^{IV}-SOMS where x = 100*[M^{IV}] / [M^{IV} + Nb]. The 20%-Na/Nb/Ti^{IV}-SOMS (SOMS-1) is the composition most readily obtained in its pure form.(*5*) Precursor sols of lower concentrations of titanium or zirconium (<20%) tend to crystallize as perovskite or illmenite upon hydrothermal treatment. However, addition of 2,4-pentadionate to the reaction mixtures provided pure samples of x%-Na/Nb/M^{IV}-SOMS (x<20%) consistently, and hence systematic compositional variation is readily achievable. (Note: The 2,4-pentadionate is not incorporated into the SOMS phases, it only aids in their formation.) Higher concentrations of the titanium (>1:4 Ti:Nb ratio) in the precursor sol results in formation of the SOMS-1 phase, along with some titanium-rich, amorphous impurities. This

suggests 20 % is the maximum possible substitution of the M^{IV} into the framework. However, syntheses with increasing Ti:Nb (up to 2:1) ratio produces larger crystals with a less needle-like morphology, as observed in figure 1.

The decreased aspect ratio of <u>SOMS-1</u> crystals with increasing titanium in the synthesis provided weakly diffracting crystals (5x8x8 μm) suitable only for data collection at an X-ray synchrotron source.(*6*) In addition to small crystal size and elongate crystal morphology, this phase has presented numerous challenges in data collection and interpretation, including the effects of non-merohedral twinning.

A variety of spectroscopic data (TGA, ICP-AES, ^{1}H solid-state MAS NMR(*7*)) led us to a fixed composition for <u>SOMS-1</u> of $Na_{16}Nb_{12.8}Ti_{3.2}O_{44.8}(OH)_{3.2} \cdot 8H_2O$, which gave a satisfactory crystallographic solution with a discrepancy index of $R_1 = 6.29$ % for the single crystal structure determination (*6*). To ensure the single crystal structure determination was representative of the bulk <u>SOMS-1</u> sample, synchrotron X-ray powder diffraction data were collected (*8*) and modeled by the Rietveld method. The excellent agreement (*8*) indicates that indeed the model derived from single crystal and powder data are equivalent. The structure of <u>SOMS-1</u> is viewed down the *b*-axis in figure 2. In this chemically-constrained model, 3.2Ti and 12.8Nb atoms per unit cell distribute statistically over two crystallographically independent Nb/Ti-sites. The occupancies of the octahedrally coordinated Na1 and Na2 sites and the square planar Na3 site were fixed at full occupancy consistent with 5:4:1 Na:Nb:Ti ratio observed by chemical analysis (ICP-AES). The geometry of the Na3 site is in fact distorted by displacements away from the square planar position in the direction of the *b*-axis, giving rise to 50% occupied sites 0.52 Å above and below the plane of the oxygen atoms. Although such coordination is unusual for Na^+, it is not unprecedented and is likely a compromise to the restricted coordination geometry provided by the framework. (*9*) The isotropic displacement parameter for this site is 11.8 $Å^2$ indicating some positional disorder, similar to that described in the structure containing 4-coordinated sodium. (*9*) The ^{23}Na MAS NMR analysis (*7*) confirmed two Na geometries in a 3:1 ratio (octahedral:distorted square planar) at −8 ± 1 ppm (octahedral) and −11 ± 2 ppm (distorted square planar).
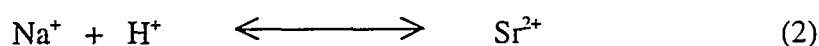
The overall architecture of SOMS-1 consists of three structural units. Edge-sharing double chains of Nb/Ti octahedra containing out-of-center atoms common to Nb/Ti chemistry run parallel to [010], and are seen in a [102] projection in figure 3. These units, when viewed along [322] are strands of the NaCl structure that often occur in vanadium, titanium and niobium oxides. The second building unit is a layer of Na-centered polyhedra consisting of edge-linked, six coordinated Na1 and Na2 atoms (figure 4). The framework then consists of sheets of these Na-layers alternating with layers containing the double chains of Nb/Ti-centered octahedra. Between the double chains resides the third structural unit, the Na3 sites.

As Na2 is coordinated to six oxygen atoms of the framework, it is less likely to ion exchange than Na1 and Na3 which both have water occupying a coordination site. ICP-AES and X-ray powder diffraction (XRPD) (7) analyses of H^+-exchanged SOMS-1 indicate that approximately 50% of the total sodium content exchanges for H^+ without disrupting the framework structure. Based on this result and possible sites for ion-exchange, the simulated powder pattern generated when half of the atoms at Na1 site and all the atoms at Na3 sites were exchanged for H^+ best explains the observed XRPD patterns. Similarly, the simulated powder pattern generated when only half of the atoms at the Na1 site were exchanged with Sr^{2+} best explains the XRPD patterns for the 20% Sr^{2+}-exchanged samples in SOMS-1. From these simulation studies, we believe that larger cations such as Sr^{2+} would substitute into only the 6-coordinate Na1 sites. Furthermore, since only half Na1 can be removed and still retain the framework structure, a maximum ion-exchange capacity of 25% only would be observed for Sr^{2+}. Whereas, smaller cations can show a maximum exchange capacity up to 50%, as all the 4-coordinate Na3 sites can be replaced in addition to half of the Na1 sites. Complete structure determinations, as well as in-depth ^1H and ^{23}Na NMR studies of Sr^{2+}, H^+ and other cation-exchanged samples are in progress, particularly to identify the site and mechanism for Sr^{2+} exchange.

5

These new <u>SOMS</u> phases are currently under rigorous investigation as tailorable ion exchanger materials for hazardous metal cleanup and sequestration. The <u>SOMS</u> phases exhibit extreme selectivity for divalent cations over monovalent cations. The distribution coefficients (K_d) for a variety of hazardous industrial metals, the alkali metals and the alkaline earth metals on the 12%-Na/Nb/Zr^{IV}-<u>SOMS</u> and <u>SOMS-1</u> phases are summarized in Table I, where K_d is defined (*10*) as the ratio of metal adsorbed onto the ion exchanger to the metal remaining in solution (*11*). Most of the divalent transition metals as well as the Ba^{2+} and Sr^{2+} are completely removed from solution by both <u>SOMS</u> phases. Selectivity of the <u>SOMS</u> phases (directly correlated with K_d) for the monovalent alkali metals is extremely low, compared to selectivity for divalent alkaline earth metals. The results compiled in Table I indicate the <u>SOMS</u> phases could be used for applications such as cleanup of nuclear waste ($^{90}Sr^{2+}$) or industrial waste streams containing toxic metals such and Cd^{2+}, Ni^{2+} or Zn^{2+}. (*12*)

Elemental analyses of <u>SOMS-1</u> following maximum exchange of Sr^{2+} gave a final Na^+:Sr^{2+} ratio of 4:1, which exactly matches the Nb:Ti ratio. The ratio of the remaining sodium (unexchanged) to the niobium is 1:1, which indicates the Na^+ and Sr^{2+} exchange in a 1:1 ratio, since the initial Na:Nb:Ti ratio is 5:4:1. Therefore; in order to maintain charge balance, a H^+ from the framework hydroxyl is necessarily exchanged along with each Na^+:

$$Na^+ + H^+ \quad \longleftrightarrow \quad Sr^{2+} \qquad (2)$$

This is confirmed by the disappearance of the OH$^-$ proton NMR resonance (+0.5 ± 0.5 ppm) in Sr^{2+}-loaded <u>SOMS-1</u> that was observed for unexchanged <u>SOMS-1</u>.

Finally, the Sr^{2+}-loaded <u>SOMS-1</u> phase undergoes direct thermal conversion to a single-phase perovskite, which has a formula of $Na_4SrNb_4TiO_{15}$. The DTA-TGA analysis of the Sr^{2+}-loaded <u>SOMS-1</u> phase, along with micrographs of 1) Sr^{2+}-loaded <u>SOMS-1</u> phase, and 2) $Na_4SrNb_4TiO_{15}$, are shown in figure 5. The weight loss between 100 – 300 °C is dehydration accompanied by structure collapse. The exothermic phase change observed at 550 °C is associated with conversion to the perovskite form. The micrographs of the

Sr^{2+}-loaded <u>SOMS-1</u> and the $Na_4SrNb_4TiO_{15}$ perovskite reveal that this phase change takes place with minimal morphology change. This thermally-induced phase change provides a means of sequestration of hazardous metals (such as radioactive Sr^{2+}), after it is selectively sorbed from solution. Perovskite (titanate-based) is a major component in the well-known SYNROC ceramic waste form for high level radioactive waste storage. (*2*) The perovskite waste-form is known to be a reliable commodity for stability in radioactive fields and in repository conditions. Since the concentration of the exchanged-in strontium exactly matches that of the framework titanium, the perovskite formed upon calcination is charge balanced without oxygen vacancies (*13*) that might reduce the durability of the resulting phase. Furthermore, there is a 99% lattice match between the $NaNbO_3$ and $SrTiO_3$ perovskites, so phase separation due to lattice mismatch is not likely. Additionally, alternative phases such as lamellar niobates, titanates, or titanoniobates (*14*) do not form. Finally, the low temperature required for this phase change, as well as the remarkable morphology preservation during this process indicates that remobilization of the strontium during heating is improbable.

To summarize, the <u>SOMS-1</u> not only selectively removes Sr^{2+} from solution, but it sorbs the necessary amount so that its thermal dehydration and phase alteration produces the most stable perovskite phase material. Based on these unique properties, it is an ideal candidate for $^{90}Sr^{2+}$ cleanup and sequestration at $^{90}Sr^{2+}$-contaminated sites. (*15*) The divalent cation selectivity and a maximum exchange which matches exactly the M^{IV} framework concentrations is likely to be a direct consequence of the substitution of the M^{IV} into the framework Nb^{5+} sites. This new class of materials also provide a unique opportunity to investigate form-function relationships of materials with ion selectivity and exchange capabilities. Additional material functionalities with respect to compositional variation are currently under rigorous investigation, so that we may fully develop and understand the "tuneability" of the <u>SOMS</u> phases. Finally, we are investigating expanding the class of materials to include: 1) phases with higher concentrations of Ti^{IV}/Zr^{IV}, 2) phases whose framework sites are substituted by other metals such as redox active metals, 3) phases with organic interstitial cations, and 4)

phases with alternative alkali metals which may occupy both framework and interstitial

sites.

References:

1. S. F. Agnew, J. G. Watkin, "Estimation of Limiting Solubilities for Non-Radioactive Ionic Species in Hanford Waste Tank Supernates" (Los Alamos National Labs, Los Alamos, NM, 1994).

2. R. G. Dosch, C. J. Northrup, T. J. Headley, *J. Am. Ceram. Soc.* **68**, 330 (1985); R. G. Dosch, T. J. Headley, P. Hlava, *J. Am. Ceram. Soc.* **67**, 354 (1984); L. Li, S. Luo, B. Tang, D. Wang, *J. Am. Ceram. Soc.* **80**, 250 (1997); S. Luo, L. Li, B. Tang, D. Wang, *Waste Management* **18**, 55 (1998); E. R. Vance, M. W. A. Stewart, G. R. Lumpkin, *J. Mater. Sci.* **26**, 2694 (1991); M. Nyman, T. M. Nenoff, B. X. Gu, L. M. Wang, R. C. Ewing, *Micro. and Meso. Mater.* **in press** (2000); M. Nyman, F. Bonhomme, D. M. Teter, T. M. Nenoff, R. S. Maxwell, B. X. Gu, L. M. Wang, R. C. Ewing, *Chem. Mater.* **accepted** (2000).

3. T. M. Nenoff and M. Nyman "A New Class of Inorganic Molecular Sieves: Sodium Niobium Metal Oxides" (Sandia National Laboratories Technical Advance # SD-6576/S-93,849, Albuquerque, NM (2000)).

4. E. Nicolas-Tolentino, Z. Tian, H. Zhou, G. Xia, S. L. Suib, *Chem. Mater.* **11**, 1733 (1999); J. Luo, Q. Zhang, A. Huang, O. Giraldo, S. L. Suib, *Inorg. Chem.* **38**, 6106 (1999); J. Luo, Q. Zhang, S. L. Suib, *Inorg. Chem.* **39**, 741 (2000).

5. Titanium (IV) isopropoxide (TIPT, 0.8 g, 2.8 mmol) and niobium (V) ethoxide (3.56 g, 11.2 mmol) were combined and ultrasounded in an airtight vial to mix thoroughly. Sodium hydroxide (6.7 g, 167.5 mmol) was dissolved in 10 ml deionized water in a 125 ml teflon liner for a Parr reactor, and the alkoxides were added while stirring vigorously. The mixture was stirred for 30 minutes, and 30 ml more water was added. The final molar ratio of water:Na:Ti:Nb of the precursor mixture was 160:12:0.2:0.8, and the pH = 13.6. The mixture was reacted in a 175 °C oven for 5 – 7 days. Approximately 2.2 grams (93% yield based on TIPT) of white, microcrystalline powder was collected by filtration.

6. Single-crystal X-ray diffraction data for $Na_{16}Nb_{12.8}Ti_{3.2}O_{44.8}(OH)_{3.2} \cdot 8H_2O$ were collected at 293 K on a Bruker SMART Platform charge couple device (CCD) diffractometer at the X3A1 beamline of the National Synchrotron Light Source (NSLS), Brookhaven National Laboratories (BNL), Upton NY, USA. Data are as follows: monoclinic *C2/c* (no. 15); $a = 16.940$ (3) Å, $b = 5.033$ (5) Å, $c = 16.466$ (3) Å; $\beta = 114.00$ (3)°, $Z = 8$, $V = 1282.6$ (3) Å^3, $d_{calc} = 3.238$ mg/m^3; $\mu = 3.351$ mm^{-1}, $7.7° < 2\theta$ (synchrotron radiation, $\lambda = 0.643$ Å) $< 46.44°$; total reflections = 2625 ; unique reflections = 1177; R[I>2σ(I)]=0.0629, R$_w$[I>2σ(I)]=0.1609; R(all data)=0.0687, R$_w$(all data)=0.1637; GooF=1.004. All initial attempts to index the unit cell using the standard SMART [Siemens, SMART. Area Detector Control Software, Siemens Analytical X-ray Instruments Inc., Madison, WI, USA, 1994.] indexing routine failed. The specimen was indexed as a non-merohedral reflection twin [A. Tripathi, V. G. Young, G. M. Johnson, C. L. Cahill, J. B. Parise, *Acta Cryst. C* **C55**, 496 (1999).], following the complete data collection, using the *GEMINI* suite of programs [V. G. Young and R. A. Sparks, *Acta Cryst. B* **in prep.** 2000]. The

orientation matrices for two twin components were determined from a set of 431 reflections. The two orientation matrices are related by the following twin law (by rows) in reciprocal space: (-100; 0-10; 001). Using the two orientation matrices, the integration program SAINT [Bruker, SAINT: Program to Integrate and Reduce Raw Crystallographic Area Detector Data, Bruker AXS, Inc., Madison, WI, USA, 1996] was used to generate two files of integrated intensities from the original frames of data. The structure was solved by SHELXS using data files generated using only the major twin component. The refinement of this file using SHELXTL [G. M. Sheldrick, SHELXTL, Bruker AXS Inc., Madison, WI, USA, 1997.] resulted in a poor refinement with unacceptable bond distances to oxygen around Nb/Ti- and Na-sites, a R value = 13.2%, and estimated high standard deviations. The overlapped reflections in the as-collected data were assigned batch scale factors (BASF) utilizing the program Twin HKL. This generated a file in which allowance was made for both exactly overlapped reflections (557) and partially overlapped reflections (2068) and these were used for the refinement of atomic parameters. The exactly overlapped reflections were placed in one group and the partially overlapped reflections were placed in six other groups depending on the degree of overlap.

7. Inductively Coupled Plasma-Atomic Emission Spectroscopy (ICP-AES) for Nb, Ti, Zr, Na, and Sr was carried out using an AtomScan-25 ICP-AES instrument, with an argon plasma flame. Samples were dissolved in HF and diluted with water. Reference samples were 10, 20 or 50 ppm of the analyzed elements. Differential Thermal Analysis-Thermogravimetric Analysis (DTA-TGA) experiments were performed on a STD 2960 TA DTA-TGA instrument with alumina as a standard for DTA. Samples (10 - 15 mg) were heated at 5 °C/min to 1000 °C with an argon flow of 20 cc/min. ^{1}H solid-state NMR was performed on a Chemagnetics CMS-300 spectrometer using a 5 mm Chemagnetic CRAMPS probe. The Br-24 pulse sequence was used to remove dipolar couplings. [D. P. Burum and W. K. Rhim, *J. Chem. Phys.* **71**, 944 (1979).] Magic Angle Spinning was applied to remove chemical shift anisotropy effects. The ^{1}H 90° pulse lengths were 1.6 μs and τ = 3.1 μs. Multiple pulse tune up procedures were followed and resolution was tested on adipic acid [D. P. Burum, M. Linder, R. R. Ernst, *J. Magn. Res.* **44**, 173 (1981).]. Spinning speeds were all set for 1.8 kHz. ^{23}Na MAS NMR analyses: ^{23}Na MAS experiments were run at 130 MHz on a Bruker DRX-500 spectrometer using a 4 mm MAS probe. Spinning speeds were set to 12 – 14 kHz. All chemical shifts were referenced to 0.1 M NaCl solutions. Excitation pulses of π/20 (1μs) and delays of 4 s were used. Deconvolutions were performed by individually fitting each spectrum to a linear combination of one narrow Gaussian peak (octahedral site) and one second order Quadrupolar broadened central transition. [*Proc. Ampere Int. Summer School*, **Vol. II**, 75 (1971).] X-ray Powder Diffraction (XRPD) data were collected on a Siemens D500 diffractometer with a Ni-filtered CuKα radiation over the angular range 5-60 ° 2θ with a step size of 0.05 ° and a counting time of 5 seconds per step. The front-loaded sample was rotated at 30 rpm during the measurement.

8. X-ray powder data (5° < 2θ < 80°, step size 0.01°, T = 298 K, λ = 1.3997 Å) for $Na_{16}Nb_{12.8}Ti_{3.2}O_{44.8}(OH)_{3.2} \cdot 8H_2O$ were collected on beamline 2.3 at the Synchrotron Radiation Source, Daresbury Laboratory, Warrington, UK. Rietveld refinement was carried out with GSAS [A. C. Larson and R. B. Von Dreele, Los Alamos National

Laboratory, New Mexico, USA] using the single crystal structural parameters as a starting model. There were no impurity or unexplained peaks in the pattern. The refinement, using a pseudo-Voigt peak-shape model [P. Thompson, D. E. Cox, and J. B. Hastings, *J. Appl. Cryst.* **20**, 79 (1987)], proceeded satisfactorily to yield refined parameters as follows: monoclinic, *C2/c* (no. 15), $a = 16.9397$ (4) Å, $b = 5.0335$ (2) Å, $c = 16.4659$ (5) Å; $\beta = 113.998$ (1)°, $V = 1282.60$ (7) Å^3, $Z = 8$, 58 variables, 565 contributing reflections, $R(F^2) = 0.1319$, $R_p = 0.1183$, $R_{wp} = 0.1495$.

9. D. Bedlivy and A. Preisinger, *Zeit. Krist.* **121**, 131 (1965).

10. Z. Zheng, C. V. Philip, R. G. Anthony, *Ind. Eng. Chem. Res.* **35**, 4246 (1996).

11. Distribution Coefficient (K_d) Determination Experiments: K_d (ml/g) $= \{[M_{ix}]/g_{ix}\}$ / $\{[M_{sln}]/ml_{sln}\}$ [M_{ix}] is the concentration of the metal adsorbed onto the ion exchanger (ix), g_{ix} is the amount of ion exchanger in grams, [M_{sln}] is the amount of metal remaining in solution and ml_{sln} is the volume of solution in milliliters. Each solution was prepared with 50 ppm metal nitrate in 10 ml of water. The solution was shook with 0.1 g ion exchanger (SOMS) at 300 rpm at room temperature for 12 hours, and subsequently filtered to remove the ion exchanger. The concentration of the metal after contact with the ion exchanger was determined by chemical analysis at Galbraith Laboratories, Inc.; Knoxville TN.

12. J. Lehto, R. Harjula, H. Leinonen, A. Paajanen, T. Laurila, K. Mononen, L. Saarinen, *J. Radioanal. Nucl.* Chem. **208**, 435 (1996); P. Sylvester and A. Clearfield, *Solvent Extraction and Ion Exchange* **16**, 1527 (1998); P. Sylvester and A. Clearfield, *Sep. Sci. Technol.* **33**, 1605 (1998); R. G. Anthony, C. V. Philip, R. G. Dosch, *Waste Management*, **13**, 503 (1993); R. G. Anthony, R. G. Dosch, D. Gu C. V. Phillip, *Ind. Eng. Chem. Res.* **33**, 2702 (1994).

13. M. T. Anderson, J. T. Vaughey, K. R. Poeppelmeier, *Chem. Mater.* **5**, 151 (1993).

14. M. Fang, C. H. Kim, T. E. Mallouk, *Chem. Mater.* **11**, 1519 (1999).

15. E. K. Wilson, *Chem. Eng. News*, 30 (September 29, 1997)); D. L. Illman, *Chem. Eng. News*, 9 (June 21, 1993).

Acknowledgements:

Figure Captions:

Figure 1. Scanning Electron Micrographs of SOMS-1 (Na$_{16}$Nb$_{12.8}$Ti$_{3.2}$O$_{44.8}$(OH)$_{3.2}$•8H$_2$O), demonstrating variation in crystal morphology with varying ratio of Nb:Ti alkoxides in the precursor mixture. An increase in crystal size, along with a decreased aspect ratio is observed with increasing titanium alkoxide in the precursor mixture. (A) Nb alkoxide:Ti alkoxide = 4:1. (B) Nb alkoxide:Ti alkoxide = 3:1. (C) Nb alkoxide:Ti alkoxide = 2:1.

Figure 2. Polyhedral representation of the structure of SOMS-1 projected along the *b*-axis. The double chains containing disordered Nb/Ti (blue) centered octahedra are connected to two layers of six coordinated Na-centered polyhedra (yellow). Na3 in distorted square planer geometry is shown as a ball and stick model (water, blue; oxygen, red; Na, yellow).

Figure 3 Polyhedral representation of the Nb/Ti octahedra along [102] in SOMS-1. The disordered octahedra (blue) have out of center Nb/Ti atoms.

Figure 4. Polyhedral representation of the structure of SOMS-1 projected along [3-21] The Na1 and Na2 polyhedra in yellow link the strands of octahedrally coordinated Nb/Ti atoms in blue.

Figure 5. Thermal conversion of Sr^{2+}-loaded SOMS-1 to SrNa$_4$TiNb$_4$O$_{15}$ perovskite. (A) DTA-TGA analysis of Sr^{2+}-loaded SOMS-1. Weight loss (TGA curve) up to 150 °C is surface water, and from 150 – 350 °C is internal, Na-bonded water (~ 5 wt. %). The exothermic phase change (DTA curve) observed at 575 °C is alteration to a perovskite phase, as confirmed by powder XRD. Scanning Electron Micrographs of Sr^{2+}-loaded SOMS-1 (B) and SrNa$_4$TiNb$_4$O$_{15}$ perovskite (C), showing virtually no morphology change accompanying this phase change.

Table I. Selectivity (K_d) of Metals on <u>SOMS</u> Phases

metal	radius in pm (6-coordinate)	20%-Na/Nb/Ti-<u>SOMS</u> (K_d, ml/g)	12%-Na/Nb/Zr-<u>SOMS</u> (K_d, ml/g)
Ba^{2+}	149	> 99,800	> 99,800
Sr^{2+}	132	> 99,800	> 99,800
Ca^{2+}	114	2300	2657
Mg^{2+}	86	226	458
Pb^{2+}	133	66,497	22,022
Cr^{3+}	94	> 99,800	> 99,800
Co^{2+}	89	> 99,800	> 99,800
Ni^{2+}	83	> 99,800	> 99,800
Zn^{2+}	88	> 99,800	> 99,800
Cd^{2+}	109	> 99,800	> 99,800
Cs^+	181	150	169
K^+	152	95	153
Li^+	90	8	35

A   20 μm   B   20 μm   C   20 μm